열경화성 복합재 로켓 방화벽의 파손 예측

이선표* · 이정윤*

Failure Prediction of Thermo-Chemically Decomposing Composite for Rocket Thermal Insulators

Sunpyo Lee* · Jung Youn Lee*

ABSTRACT

The theory developed in a preceding paper [1] for poroelastic composite material behavior under thermal and gas diffusion is applied to thermo-chemical decomposition of a carbon-phenolic composite rocket nozzle liner under typical operating conditions. Specifically, the structural component simulated is the cowl ring for which distributions of pressure in the material pores, temperature and across-ply stress are presented. The results for particular composite designs show that across-ply failure occurs due to tensile stress in the material which is indicative of plylift. This prediction corroborates observations of plylift in a nozzle cowl. Simulations suggest designs to avoid plylift in the cowl zone.

초 록

카본-페놀릭 복합재로 제작된 로켓 방화벽이 운전조건 하에서 열-화학적 분해되는 것을 해석하기 위해 [1]의 논문에 기술된 열 및 기체확산을 수반하는 다공 탄성 복합재료의 거동이론을 적용하였다. 해석 대상의 구조 부재는 카울 링이며, 재료 내의 압력, 온도 및 층간 응력이 제시되었다. 특정 조건의 복합재 구조에 대한 해석의 결과는 재료 내의 발생하는 인장응력에 의해 플라이리프트를 나타내는 층간파손을 나타낸다. 해석 결과는 실제 구조의 파손과 모양 및 위치가 일치한다. 이 방법은 플라이리프트와 같은 파손을 피하기 위한 설계에 적용될 수 있다.

Key Words: Solid Rocket Motor(고체로켓모터), Carbon-Phenolic(카본페놀릭), Thermal Insulator(방화벽)

1. Introduction

In the aerospace industry, carbon-phenolic composites have been used as thermal insulation liners to protect the structure from

† 2005년 3월 31일 접수 ~ 2005년 6월 8일 심사완료
* 정회원, 경기대학교 기계시스템디자인공학부
연락저자, E-mail: splee@kyonggi.ac.kr

heat generated in rocket motor nozzles. Heat transferred into the insulation is convected through the porous material away from the structure into the motor exhaust stream by gases generated by decomposing phenolic. However, improper design of the material-structural system can restrict this gas flow sufficiently to build excessive pressure in the pores of the material causing it to fail. Indeed, after motor operation, three kinds of failure modes have been observed: (1) plylift, an extensive separation between adjacent plies in the charred layer, (2) pocketing, characterized by deep holes in the charred layer formed by exploding chunks of material and (3) wedge out, a failure in the ring-to-ring insulation joint area. The failure treated here is plylift or ply delamination. The present work is motivated by a need for analysis in order to design insulation liners that will not fail in this manner.

In a preceding paper [1], we developed a revised theory to solve a coupled set of different equations governing the mechanical response of poroelastic anisotropic materials during thermal decomposition and an axisymmetric finite element formulation to simulate the process in space and time. The method was then applied to experiments of carbon-phenolic materials in order to deduce all material properties necessary to the theory. After doing this, numerical simulation of these experiments demonstrated excellent agreement with experimental data. With this foundation complete, we apply the simulator to a structure.

In this paper, the behavior of a carbon-phenolic cowl ring segment of a solid rocket motor thermal insulator is investigated because the most common failure mode is plylift and it has been observed to occur in the cowl ring cap of the insulation liner. This zone is analyzed for a structure composed of dry material, an idealized situation. However, the results predict plylift for the design found in the observed specimen. Through further analysis, composite layup designs are suggested to prevent its occurrence. Layups within this range have been adopted in practice.

2. Insulator Configuration

Carbon-phenolic insulation liners are processed as tape-wrapped rings, mounted in series and bonded to the metallic housing during nozzle assembly. To build a tape-wrapped composite ring, the tape is cut into strips and then the strips are sewn together end-to-end to make a long discontinuous curved strip of tape. This strip is wrapped around a tapered mandrel so that it is less apt to fold and wrinkle. Multiple wraps form the ring. After the resin sets, the ring is removed from the mandrel.

There are two typical layups which form the tape: 0/90 and +45/-45. The 0/90 layup is generally orthotropic and the +45/-45 layup is monoclinic with respect to tape coordinates since the material properties in fill and warp directions are, in reality, different. However in this paper it is assumed that the properties in fill and warp directions are the same so that both type tapes are isotropic in the plane. For an axisymmetric problem, the tape used to form the construction should be orthotropic in the local (tape) coordinates and thus, when transformed to the global (cylindrical) coordinates, the construction is

monoclinic with respect to the r, z-plane, the plane of material symmetry. This is the most general configuration possible for an axisymmetric problem [2].

The constitutive relations for a gas-filled orthotropic poroelastic tape are

$$\{\tau'\} = [C'](\{e'\} - \{\beta'\}T - \{\alpha'\}p) \qquad (1)$$

where the (′) represents quantities in tape coordinates. The fields τ, e, T and p are sufficiently defined below in cylindrical coordinates and $[C']$ is a 6×6 matrix populated as usual. $\{\alpha'\}$ and $\{\beta'\}$ are 6×1 matrices and generate no shear (last three elements are zero).

For analysis of axisymmetric structures, it is necessary to transform quantities from the orthotropic to monoclinic configuration. Referring to Fig. 1, the construction in cylindrical coordinates r, θ, z is formed by wrapping strips of tape in local coordinates l, t, n such that l is taken approximately parallel to θ (strips of tape (l) are sewn along θ), oriented so that ply angle lies between direction t and axial direction z. The transformation between coordinates is written in terms of the direction cosines as

$$\begin{Bmatrix} b_r \\ b_\theta \\ b_z \end{Bmatrix} = \begin{bmatrix} 0 & s & c \\ 1 & 0 & 0 \\ 0 & c & -s \end{bmatrix} \begin{Bmatrix} b_l \\ b_t \\ b_n \end{Bmatrix} \qquad (2)$$

where $s = \sin\phi$, $c = \cos\phi$ and b_i represents a unit basic vector in direction i.

Using this relation, the material properties are transformed into cylindrical coordinates and the constitutive equation becomes

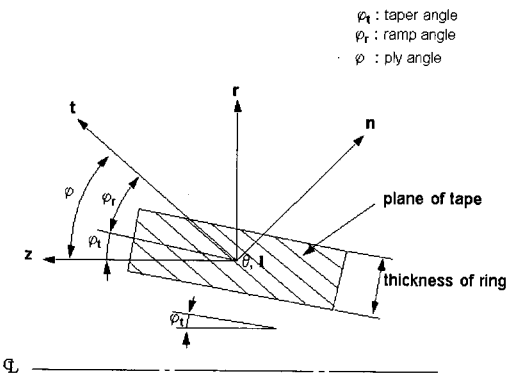

Fig. 1 Section geometry showing tape (l, t, n) and cylindrical (r, θ, z)coordinates. Note: θ, l point into the paper and t, n are within and normal, respectively, to the plane of the tape

$$\begin{Bmatrix} \tau_1 \\ \tau_2 \\ \tau_3 \\ \tau_4 \\ \tau_5 \\ \tau_6 \end{Bmatrix} = \begin{bmatrix} C_{11} & C_{12} & C_{13} & 0 & 0 & 0 \\ C_{21} & C_{22} & C_{33} & 0 & 0 & 0 \\ C_{31} & C_{32} & C_{33} & 0 & 0 & 0 \\ 0 & 0 & 0 & C_{44} & 0 & C_{46} \\ C_{15} & C_{25} & C_{35} & 0 & C_{55} & 0 \\ 0 & 0 & 0 & C_{64} & 0 & C_{66} \end{bmatrix} \times$$

$$\left(\begin{Bmatrix} e_1 \\ e_2 \\ e_3 \\ e_4 \\ e_5 \\ e_6 \end{Bmatrix} - \begin{Bmatrix} \beta_1 \\ \beta_2 \\ \beta_3 \\ 0 \\ \beta_5 \\ 0 \end{Bmatrix} T \right) - \begin{Bmatrix} \alpha_1 \\ \alpha_2 \\ \alpha_3 \\ 0 \\ \alpha_5 \\ 0 \end{Bmatrix} p \qquad (3)$$

where e_i are the usual linear total strain components in terms of displacements u, w in the r, z directions. C_{ij} are the elastic moduli, β_i the coefficients of thermal expansion acting upon temperature change T, α_i are the Biot's constants acting upon the pore pressure p and τ_i are the total stress. Explicit expressions for the elements in the above matrices are found in Lee's dissertation [2].

(Transformation of the Biot forms of the above are given in Cook, et al. [3].)

In order for this to conform to axisymmetric conditions, $e_4=e_{\theta z}=0$ and $e_6=e_{r\theta}=0$ are imposed, hence $\tau_4=\tau_{\theta z}=0$ and $\tau_6=\tau_{r\theta}=0$, which eliminates one of three equations of motion. Notably $e_5=e_{rz}$ and $\tau_5=\tau_{rz}$ are nonzero, therefore even for the simplest configurations the problem is not uniaxial.

3. Cowl Ring Cap Analysis

When the motor is ignited, the nozzle liner material is heated very rapidly and decomposition occurs to form a growing char layer as the thermal front moves from the surface exposed to exhaust gas into the material. Simultaneously pressure rises in the pores of the material as decomposition gases are generated. The model for the analysis of a portion of the cowl ring is designed to simulate such ignition conditions.

3.1 Finite Element Model and Boundary Conditions

To implement the finite element method, a coupled chemical-thermal-structural code has been written. The code is written in the FORTRAN language and has been compiled on an IBM-PC within the Windows XP environment.

In general, a system as complicated as this one is subject to many phenomena difficult to model. We impose the following assumptions:

Pressure dependence of reactive gases is not considered and the material is dry. This means condensation of reactive gases and water vapor is not considered.

Heat from the exhaust gas is supplied to the exposed insulation wall by prescribing a convective heat flux q as a function of temperature in the simple form

$$q = h_{conv}(T_g - T_s) \tag{4}$$

where the unknown wall temperature T_s is updated at every time step. The convection coefficient h_{conv} and wall temperature T_g are chosen to be constants: this ignores the many complicated phenomena occurring at the ablating, eroding, gas-emitting surface interacting with a particle-laden flow. Based upon discussions with investigators familiar with fluid dynamical aspects of the problem, the temperature of the exhaust gas is set to 3500 Kelvin, the maximum operating temperature, and the convection coefficient is set to 500 W/K-m^2.

Material constants, particularly those dependent upon material response, are set to those determined in [1]. In other words, this in situ problem is sufficiently similar to the experimental problems to make the results obtained here meaningful.

Fig. 2 Section of an actual fired cowl zone showing plies lifting approximately 0.8 cm to 1.4cm from the exposed surface at bottom

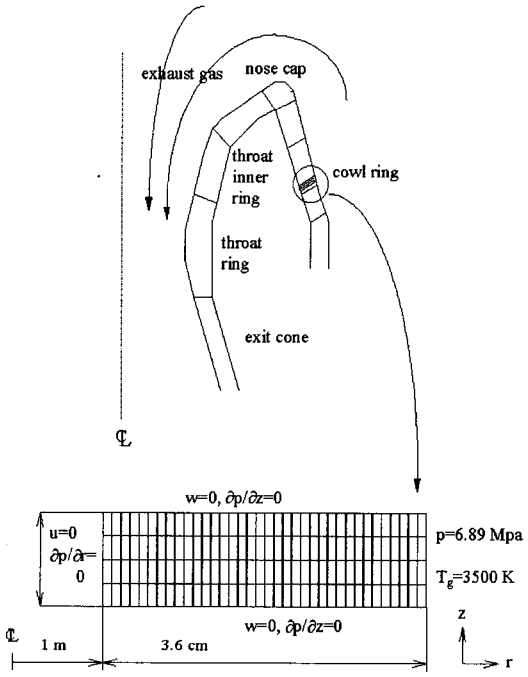

Fig. 3 Schematic illustration of a rocket nozzle structure and finite element model for cowl zone

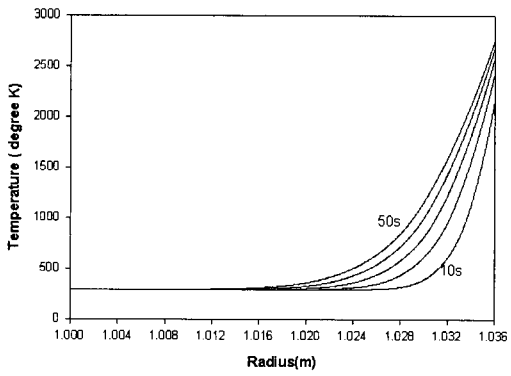

Fig. 4 Pore pressure profiles in cowl zone shown every 10s from 10s to 50s

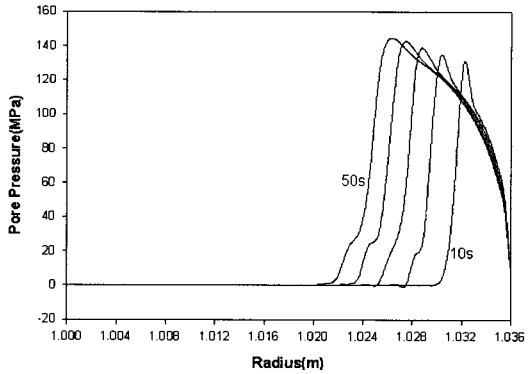

Fig. 5 Variation of temperature profiles in cowl zone shown every 10s from 10s to 50s.

3.2 Observation for model

A photograph of a specimen cut from a fired rocket nozzle is shown in Fig. 2. It is observed that plylift occurs from 0.8 cm to 1.4 cm from the surface exposed to the exhaust gas in a fired cowl ring for which the ply angle is 25. This section exhibits delamination and, in the extreme, buckling of plies apparently caused by in-plane compressive stress. To develop the model for this region, a schematic illustration of a solid rocket motor nozzle and the finite element model for a cowl ring section is shown in Fig. 3. The taper of the actual section modeled is 10 degrees; we assumed zero for the ring taper angle ϕ_t .

The model is loaded at the outer radius by a constant exhaust gas pressure of 6.89 MPa (1000 psi). Since the cowl ring is backed by much stiffer components at the inner radius, the radial displacement u at that point is set equal to zero and the impermeable condition is given there.

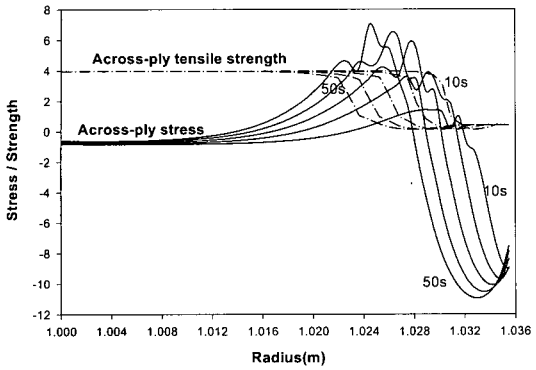

Fig. 6 Comparison of across-ply stress and across-ply tensile strength shown every 10s from 10s to 50s.

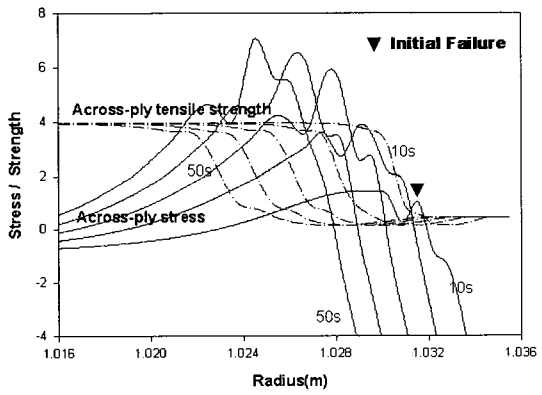

Fig. 7 Comparison of across-ply stress and across-ply tensile strength shown every 10s from 10s to 50s (Zoom).

Also, since the cowl ring is long in the axial z-direction, only 1 cm of the cowl ring in the z-direction is modeled and axial displacements (w) are set equal to zero at z = 0 and z = 1 cm (plane strain condition) and impermeable conditions are given there. The simulations employ 172 bilinear, axisymmetric quadrilateral finite elements uniformly distributed (44 nodes radially by 5 axially).

It should be noted that the finite element model for the cowl zone is restrained in the axial z-direction similar to the RTG test simulation model. Hence it conforms with assumption.

3.3 Results : Prediction of Plylift Location.

Figures 4, 5 and 6 display pore pressure, temperature and across-ply stress, respectively, versus radial position (hot gas exposed surface on the right) for time values running from 10s to 50s after rocket ignition in 10s intervals. As time proceeds, the peak of pore pressure and the temperature move deeper into the material such that the magnitude of the pressure peaks vary with time from 133MPa to 147MPa and occur where the temperature is 670±80 K. This temperature range corresponds with that for pore pressure peaks found for the restrained thermal growth tests [1].

Across-ply total stress (τ_n) and tensile strength are plotted together in Fig. 6. The tensile strength of the material varies because it is a function of degree-of- char. As time proceeds, the increasing temperature front moves into the material driving up the pore pressure and the across-ply stress while the across-ply tensile strength degrades. At 10s the across-ply stress crosses the across-ply tensile strength at r = 1.031 m which is 0.5 cm from the exposed surface and across-ply failure occurs. At 50 seconds, the failure zone stretches inward from r = 1.028 m to r = 1.022 m. This is better viewed in Fig. 7 which zooms in on the region of interest. Although the simulation predicts failure closer to the exposed surface than the observed failure, the result is reasonable considering the assumptions made to solve the problem.

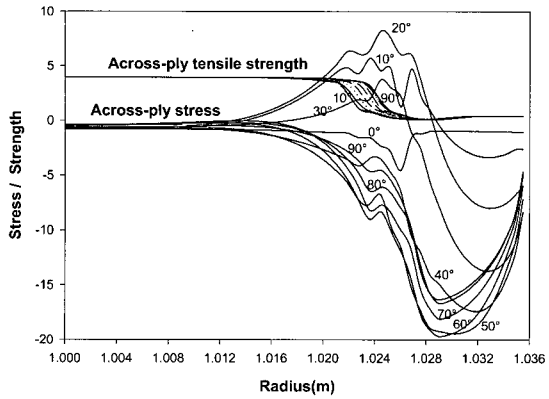

Fig. 8 Comparison of across-ply stress profiles in the cowl zone at t = 50 seconds when various ply angles are used in the analysis

It may seem more appropriate to compare the mechanical stress $[C](\{e\}-\{\beta\}T)$ to the strength, but the strength was measured prior to application of Biot theory [4], hence no account could have been taken of the pore pressure in the material: consequently, we believe it was the total stress that was measured.

3.4 Design of the Cowl Zone

One way to prevent plylift is to change the ply angle in order to reduce across-ply tension. The across-ply stress profiles in the cowl zone at 50 seconds are plotted in Fig. 8 for various ply angles. The across-ply tensile failure occurs at ply angles from 7 to 32.The magnitude of the across-ply stress peak decreases at angles greater than 20. For ply angles greater than or equal to 33, the across-ply stresses are totally compressive. Hence tensile failure, i.e., plylift, can be avoided. It appears that the ply angle strongly effects the performance of the rocket insulation liner.

4. Conclusion

The axisymmetric theory [1] is applied to a carbon-phenolic cowl region of a rocket nozzle liner under operating conditions. As a result, a plausible failure mechanism for plylift is revealed and designs to avoid plylift are suggested.

For the cowl zone, the location and temperature at which across-ply failure has been observed corresponds with that predicted by the numerical simulation.

Various ply angles in the cowl zone have been examined and it is found that the use of appropriate ply angles in this region can prevent plylift by reducing the maximum across-ply stress. Hence fail-safe designs appear possible for the duration of rocket flight.

References

1. S. Lee and J. Y. Lee, "Analysis of thermo Chemically Decomposing Composites for Rocket Thermal Insulators," Journal of the Korean Society of Propulsion Engineers, Vol. 5, No. 4, 2001, pp. 1-11.
2. S. Lee, "Coupled Finite Element Analysis of Decomposing Poroelastic Polymeric Composites and Structures with Subsequent Thermal and Gas Diffusion," Ph. D. Dissertation, The Pennsylvania State University, 1993
3. R.D. Cook, D.S. Malkus and M.E. Plesha, Concepts and Applications of Finite Element Analysis, Wiley, New York, 1989
4. M.A. Biot, "General Theory of Three-Dimensional Consolidation," Journal of Applied Physics, Vol. 12, 1941, pp.155-164.